TITLE

Proof of concept study deploying CRISPR inhibition and activation opens key avenues for systematic biological exploration in zebrafish.

AUTHORS

Nelson B. Barrientos[1], Elyse A. Shoppell[1], Rachel J. Boyd[1], Valeria C. Culotta[2], Andrew S. McCallion[1,3*]

AFFILIATIONS

[1]McKusick-Nathans Department of Genetic Medicine, Johns Hopkins University School of Medicine, Baltimore, MD 21205, USA

[2]Department of Biochemistry and Molecular Biology, Johns Hopkins University Bloomberg School of Public Health, Baltimore, MD 21205, USA

[3]Department of Medicine, Johns Hopkins University School of Medicine, Baltimore, MD 21205, USA

[*] Corresponding author

Corresponding author's email: andy@jhmi.edu

ABSTRACT

The application of CRISPR interference (CRISPRi) and CRISPR activation (CRISPRa) technologies in zebrafish has the potential to expand its capacity for the study of gene function significantly. We report proof-of-principle data evaluating transient expression of a codon optimized CRISPRi/a system for zebrafish across established pigmentary and growth phenotypes. A codon-optimized and catalytically inactive *cas9* gene (*dcas9*) was cloned upstream of codon-optimized Krüppel associated box (KRAB) and methyl-CpG binding protein 2 (MeCP2) for CRISPRi, and VP64 for CRISPRa. To validate CRISPRi, we targeted key genes in melanocyte differentiation (*sox10, mitfa,* and *mitfb)*; and melanin production (tyrosinase; *tyr*). Microinjection of CRISPRi mRNA and single guide RNAs (sgRNAs) targeting the *tyr* promoter or 5'-UTR resulted in larvae with hypopigmented epidermal melanocytes. CRISPRi-mediated targeting of the promoters or 5'-UTR of transcription factors mitfa and mitfb also results in pronounced hypopigmentation of epidermal melanocytes (*mitfa*), and RPE (*mitfb*). Also, CRISPRi targeting of the *sox10* promoter results in hypopigmentation of both epidermal melanocytes and RPE consistent with its role upstream of *mitfa* and *mitfb*, and *tyr*. Finally, we tested both CRISPRi/a to modulate a single gene to yield hypomorphic and hypermorphic effects, selecting *mrap2a* as our target. This gene regulates energy homeostasis and somatic growth via inhibition of the melanocortin 4 receptor gene (*mc4r*). We demonstrate that inactivating or activating *mrap2a* with CRISPRi/a significantly decreases or increases larval body length, respectively. We demonstrate that CRISPRi/a can modulate control of zebrafish gene expression, facilitating efficient assay of candidate gene function and disease relevance.

KEYWORDS:

Zebrafish, CRISPR-activation, CRISPR-inhibition

INTRODUCTION

Zebrafish (*danio rerio*) are a powerful model system in which to study functional components of vertebrate genomes. Comparative genomics analyses have shown that 61.5% of mouse protein-coding genes and 71% of human protein-coding genes have at least one zebrafish orthologue[1,2]. Additional features, including short generation time, high fecundity, external fertilization, and embryonic transparency, have distinguished zebrafish as a desirable model system in which to examine developmental processes. As such, zebrafish have been widely used to study the biological relevance of regulatory elements[3–6], and human disease-associated genes[7–14].

Emerging technologies for transgenesis and genome engineering, such as such as Gal4-UAS[15]; Tol2-transposase transgenesis[3]; Zinc Finger Nucleases[16]; and transcription activator-like effectors (TALENs)[17] have been developed and rapidly implemented in zebrafish. Over the last decade, zebrafish have also been shown to be amenable to CRISPR-Cas-based genomic engineering applications, including targeted mutagenesis, base editing, and generation of knock-in and knockout models[18–22]. More recently, the emergence of CRISPR interference (CRISPRi) and activation (CRISPRa) have presented additional opportunities to explore functional components of vertebrate genomes. CRISPRi/a involves the fusion of transcriptional effectors to a catalytically inactive, or “dead” Cas9 (dCas9). CRISPRi employs a transcriptional repressor, such as a Krüppel associated box (KRAB) domain and methyl-CpG binding protein 2 (MeCP2)[23,24], while in the case of CRISPRa, a transcriptional activator, such as VP64, is fused to the dCas9[25]. To date, the CRISPRi/a systems have seen limited application in zebrafish[26], whereas they have been more rapidly employed in mammalian organisms to target human disease-relevant genes[27–29].

Here, we report initial experiments in the development and evaluation of zebrafish codon-optimized zdCas9-KRAB-MeCP2 and zdCas9-VP64 CRISPR systems. We present a systematic

evaluation of these modified proteins in functional proof-of-concept experiments by targeting two easily scored phenotypes: zebrafish pigmentation and somatic growth. In addition to providing visual confirmation of the efficacy of both CRISPRi and CRISPRa, these two model phenotypes and their corresponding pathways are well-characterized and are involved in human disease.

Specifically, we chose to test our CRISPRi system by targeting genes involved in melanocyte differentiation and pigmentation, *sox10 (SRY-box transcription factor 10)*, *mitfa (melanocyte inducing transcription factor a)*, *mitfb*; and the gene for the rate determining enzyme in pigmentation, *tyr (tyrosinase)*. At approximately 16 hours post fertilization (16 hpf), *sox10* directly activates *mitfa* and *mitfb* promoters to stimulate downstream genes involved in melanocyte differentiation; and activates *tyr*, to induce melanin production by 24 hpf[30–32]. In the developing zebrafish embryo, *mitfa* and *mitfb* are co-expressed in the retinal pigment epithelium, whereas only *mitfb* is expressed in the zebrafish epiphysis and olfactory bulb, and only *mitfa* is expressed in neural crest cells[31,33,34]. We hypothesize that independently targeting each of these four genes with functional CRISPRi will yield a visible reduction in zebrafish pigmentation. In the case of *sox10,* we expect to see marked reduction in pigmentation globally due to its role in melanocyte cell fate and activation of *mitfa/b* and *tyr* to promote melanin production in zebrafish and other vertebrates[35,36]. Due to its role in multiple stages of melanocyte differentiation and its function as a transcription factor, silencing *mitfa* is expected to result in a hypopigmentation phenotype throughout the body[37]. Similarly, silencing *mitfb* is expected to delay melanocyte differentiation in the retinal pigment epithelium (RPE) and lead to areas of reduced pigmentation[33,38]. Lastly, we hypothesize that targeting *tyr* will result in hypopigmentation of melanocytes throughout the zebrafish body[30,35,39,40]. Zebrafish melanocytes have been extensively studied by our group and others[4,6,41,42], and targeting genes in this pathway is highly relevant to the study of human disease, including melanoma[43–45], Waardenburg Syndrome[46,47], microphthalmia, and Hirschsprung's disease[48,49].

101 For our CRISPRa system, we chose to target *mrap2a* (*melanocortin receptor accessory*
102 *protein 2a*), which has been found to inhibit the transcription of the *melanocortin-4 receptor*
103 (*mc4r*)[50]. As a corollary, we hypothesize that CRISPRa targeting the *mrap2a* locus will amplify the
104 inhibition of *mc4r* and promote visible growth phenotypes in zebrafish larvae. This is supported
105 by evidence in human patients, wherein autosomal dominant loss of function mutations in *MCR4*
106 results in severe childhood-onset obesity[51,52]. By contrast, we hypothesize that effective CRISPRi
107 targeting of *mrap2a* will promote *mc4r* inhibition and result in diminished zebrafish growth
108 consistent with reported morpholino-based knock-down experiments [50].
109 Ultimately, we outline the development of zebrafish-optimized zdCas9-KRAB-MeCP2 and
110 zdCas9-VP64 CRISPR constructs. We establish their utility for efficient screening of candidate
111 gene function and disease relevance. Ongoing work in the lab will establish stable transgenic
112 lines expressing these proteins to facilitate rapid and systematic screening of gain and loss of
113 gene function targeting custom guide RNAs (gRNAs) to promoters, 5'-UTR, or cell-dependent cis-
114 regulatory elements of selected candidate genes.
115

116 METHODS
117

118 **Generation of catalytically inactive Cas9 plasmid vector**
119 The WT zebrafish optimized Cas9 within the plasmid vector pT3TS-nCas9n (Addgene
120 #46757) was mutated to produce a catalytically inactive dead Cas9 (dCas9). The DNA sequence
121 corresponding to the RuvC-like and HNH nuclease domains of the Cas9 protein were modified
122 by inducing a change from Aspartic acid to Alanine at position 10 (D10A), and a change from
123 Histidine to Alanine at position 839 (H839A). This was accomplished by implementing the
124 NEBuilder HiFi DNA Assembly (Cat. # E5520S) protocol using oligonucleotides primers
125 (Supplemental Table 1) generated using the NEBuilder Assembly Tool (v.2.10.1). The modified

126 plasmid vector was then transformed into NEB 5-a competent *E. coli* cells (Cat. # C2987I) and
127 later mini-prepped using NEB Monarch Plasmid Miniprep Kit (Cat. # T1010L). The plasmid vector
128 generated was named pT3TS-ndCas9n.
129
130 **Codon Optimization of KRAB-MeCP2 and VP64 domains for zebrafish usage**
131 The DNA sequence for the KRAB-MeCP2 repressor was obtained from the dCas9-KRAB-
132 MeCP2 plasmid vector (Addgene #110821); while the DNA sequence for the VP64 activator was
133 obtained from the dCas9-VP64-GFP plasmid vector (Addgene #61422). The codon optimization
134 tool from IDT was used to optimize these sequences for zebrafish. The KRAB-MeCP2 repressor
135 sequence (1,263 bp) containing an SV40 NLS before and after KRAB was optimized and ordered
136 as a gBlocks HiFi Gene Fragment. The VP64 activator sequence (225 bp) containing an SV40
137 NLS before VP64 was optimized and ordered as a gBlocks Gene Fragment.
138
139 **CRISPRi/a plasmid construct generation and *in vitro* transcription**
140 The codon optimized KRAB-MeCP2 repressor and VP64 activator were cloned into the
141 pT3TS-ndCas9n plasmid vector containing a catalytically inactive dCas9 sequence. Cloning was
142 carried out by employing NEBuilder HiFi DNA Assembly (Cat. # E5520S) using oligonucleotide
143 primers (Supplemental Table 2) that overlapped both the target region of the plasmid vector and
144 the optimized sequences. Once the optimized sequences had been cloned in, the plasmid
145 constructs were transformed into NEB 5-a competent *E. coli* cells (Cat. # C2987I) and later mini-
146 prepped using NEB Monarch Plasmid Miniprep Kit (Cat. # T1010L). The plasmid constructs
147 generated were named zdCas9-KRAB-MeCP2 and zdCas9-VP64 for CRISPRi and CRISPRa,
148 respectively.
149 The restriction enzyme XbaI (NEB Cat # R0145) was used to linearize the CRISPRi/a
150 plasmid constructs. Subsequently, *in vitro* transcription of the d*Cas9* gene plus the repressor or
151 activator was performed by employing the mMessage mMachine T3 Transcription kit (Cat. #

152 AM1348). RNA was recovered by using the RNA Clean-up protocol from the Qiagen RNeasy Mini
153 Kit (Cat. # 74104) and stored at -80°C.
154
155 **Designing targeted gRNAs for CRISPRi/a**
156 Multiple single guide RNAs (sgRNAs) were designed to target the promoter or 5'-UTR of
157 the various genes in the zebrafish. All sgRNAs followed a core **5'-N18-3'**[53] sequence and were
158 designed using the online tool CRISPOR (PMID: 29762716). At the 5' end of the forward
159 oligonucleotide, the nucleotides 5'-TAGG-3' were added. At the 5' end of the reverse
160 oligonucleotide (reverse complement of N18 sequence), the nucleotides 5'-AAAC-3' were added.
161 The final form of the oligonucleotides was 5'-TAGG-N18-3' for the forward oligo; and 5'-AAAC-
162 N18RevCompl-3'. The oligo primers for each sgRNA were ordered from IDT (Supplemental Table
163 3). Oligonucleotide primers were first annealed and subsequently cloned into the pT7-gRNA
164 plasmid vector (Addgene #46759) containing a gRNA scaffold, according to restriction enzyme
165 cloning protocol specifications from previous studies[54]. After cloning, each plasmid construct
166 generated for each sgRNA was transformed into NEB 5-a competent *E. coli* cells (Cat. # C2987I)
167 and later mini-prepped using NEB Monarch Plasmid Miniprep Kit (Cat. # T1010L). Linearization
168 of these constructs was performed using the restriction enzyme BamHI-HF (NEB Cat # R3136).
169 The linear DNA was purified using the Zymo Research DNA Clean & Concentrator-5 protocol
170 (Cat. # D4013). Subsequently, *in vitro* transcription of linear DNA was performed using the
171 Thermo Fisher MEGAshortscript T7 Kit (Cat. # AM1354) or the NEB HiScribe T7 High Yield RNA
172 Synthesis Kit (Cat. #E2040S). After in vitro transcription, RNA was recovered by using the RNA
173 Clean-up protocol from the Qiagen RNeasy Mini Kit (Cat. # 74104) and stored at -80°C.
174
175 **Zebrafish husbandry and microinjections of one-cell stage embryos**
176 The day before injections, adult AB zebrafish (ZFIN ID: ZDB-GENO-960809-7) crosses
177 were set up in tanks with dividers at a ratio of 2:1 or 3:2 females per male. The morning of

178 injections and when the lights came on, the dividers were removed to allow for mating among
179 zebrafish. Zebrafish embryos were injected during the first 15-20 mins after being collected to
180 ensure injection occurred at the one-cell stage. The mixture injected to the embryos contain 300
181 ng of CRISPRi/a mRNA, 150 ng of sgRNA mRNA, 0.5 µl of Phenol Red, and Nuclease Free Water
182 up to 6 µl. After microinjections, zebrafish embryos were incubated at 25 °C in E3 embryo medium
183 provided by Johns Hopkins FinZ Zebrafish Core Center.
184

185 **Zebrafish measurement and image collection**

186 All zebrafish larvae used for measurements or image collection were staged according to
187 anatomical hallmarks described in Kimmel et al [55]. Larvae were anesthetized using ethyl-3-
188 aminobenzoate methanesulfonate salt (Tricane/MS-222; Sigma Aldrich #E10521) prepared at a
189 concentration of 4 mg/mL using 1 M Tris (pH 9, 4% v/v). The Nikon AZ100 Multizoom fluorescent
190 microscope was used for both measurements and image collection at a ratio of 3.22 µm/px. For
191 all images, zebrafish larvae were suspended in 3% Methyl Cellulose (Sigma Aldrich #M0387)
192 solution.

193 RESULTS
194

195 **CRISPRi modulates tyrosinase expression and its effect is observable between the prim**
196 **20-25 stages.**

197 To determine the functional capacity of zebrafish codon-optimized CRISPRi (Fig 1A), one-
198 cell stage zebrafish embryos were injected with CRISPRi mRNA and target sgRNAs. A CRISPRi
199 assay for zebrafish provides an opportunity to ask questions regarding the impact of titrating
200 downwards the expression of target genes, in evaluation of their normal biological role. As part of
201 a series of proof-of-concept experiments, we designed sgRNAs targeting the promoter region and

202 5'-UTR of the tyrosinase (*tyr*) gene, predicting that inhibition would lead to diminished larval
203 pigmentation, similar to established loss of function studies at this locus[30,32,40].

204 Initially, sgRNAs were designed to target the *tyr* promoter or 5'-UTR (Methods) and one-
205 cell embryos (n ≥ 200) were injected with CRISPRi (300 ng/µl) and a cocktail of all five sgRNAs
206 (150 ng/each). Zebrafish larvae assayed within the prim 20-25 stages (33-36 hpf) displayed
207 marked reduction in pigmentation of melanocytes (Fig 1B), consistent with phenotypes arising
208 from loss of function alleles in zebrafish[30] and other vertebrates[39]. By contrast, larvae receiving
209 only the CRISPRi mRNA (n ≥ 200) or uninjected controls (n ≥ 200), displayed no diminution in
210 melanization at these stages. As expected, the observed suppression of tyr dissipated over time,
211 and by the pec-fin stage (60 hpf), melanization was indistinguishable between controls and those
212 larvae receiving CRISPRi and the cocktail of all sgRNAs.

213 We next tested if delivery of each individual *tyr* sgRNAs could similarly silence
214 transcription of *tyr* and reduce melanin production. At least one of the five sgRNAs that we tested,
215 sgRNA4 targeting the promoter, efficiently modulated *tyr* expression (Supp Fig 1), resulting in
216 hypopigmentation within prim 20-25 (33-36 hpf). We used this sgRNA to assess the optimal
217 concentration of CRISPRi + sgRNA and injected n ≥ 200 larvae each with 100 ng/µl, 300 ng/µl,
218 and 500 ng/µl of sgRNA4. Our data suggests no advantage to injection of levels in excess of 300
219 ng/µl of sgRNA (Supp Fig 1).

220 These results demonstrate the effectiveness in modulating *tyr* by employ of our zebrafish
221 codon-optimized CRISPRi and selected individual or pooled sgRNA targeting the gene's
222 promoter. To build on these observations, we sought to confirm them through the manipulation of
223 other key pigment genes that are known to regulate *tyr*.

224

225 **CRISPRi modulates melanin production upon targeting of *mitf* genes.**

226 In light of our results modulating *tyr* expression, we next tested if we could induce its
227 silencing by targeting the genes encoding the transcription factors mitfa and mitfb. The *mitf* genes

228 play critical roles in pigmentation throughout vertebrates, targeting tyrosinase during early
229 development[35,56]. We designed sgRNAs to target the promoter and 5'-UTR regions of the *mitfa*
230 and *mitfb* genes, predicting that, as with known loss-of-function (LoF) alleles[34,56], titrating activity
231 of these transcriptions factors would result in reduced activation of tyrosinase in melanocytes
232 throughout the body (*mitfa*) and in the retinal pigment epithelium (*mitfa* and *mitfb*).

233 Four sgRNAs were designed to target the *mitfa* promoter (Methods). As before, zebrafish
234 one-cell embryos (n ≥ 200) injected with CRISPRi (300 ng/µl) and a cocktail of all *mitfa* sgRNAs
235 (150 ng/each) displayed marked reduction in pigmentation of melanocytes, assayed within prim
236 20-25 (33-36 hpf) (Fig 2a). This is consistent with prior *mitfa* LoF studies[57] where failure to
237 express *mitfa* prevents the production of melanocyte precursors, leading to reduced global
238 pigmentation in zebrafish larvae. In contrast, no reduction in pigmentation was observed in larvae
239 receiving only the CRISPRi mRNA (n ≥ 200) or uninjected controls (n ≥ 200) (Fig 2A). Additionally,
240 individual *mitfa* sgRNAs targeting the promoter or 5'-UTR effectively silenced *mitfa,* resulting in
241 marked reduction of melanin production within prim 20-25 (33-36 hpf) (Supp Fig 2). Silencing of
242 *mitfa* dissipated over time and by the pec-fin stage (60 hpf), melanization was similar between
243 controls and injected larvae (Fig 2A, Supp Fig 2).

244 For *mitfb,* five sgRNAs were designed to target the promoter and 5'-UTR (Methods), and
245 one-cell zebrafish larvae (n ≥ 200) were injected with CRISPRi (300 ng/µl) with or without a
246 cocktail of all *mitfb* sgRNAs (150 ng/each). Injected larvae were assayed between prim 20 (33
247 hpf) and the pec-fin (60 hpf) stages for differences in melanization in the RPE and compared with
248 uninjected controls (n ≥ 200) at the same developmental time. RPE morphogenesis starts at
249 around the 14-16 somite stage (16 hpf) and by the prim 15 stage (30 hpf), a single monolayer
250 RPE has formed and pigmentation is initiated[58]. Between prim 20-25 (33-36 hpf), although control
251 larvae did not show a fully pigmented RPE, larvae injected with CRISPRi and gRNAs showed a
252 noticeable hypopigmentation phenotype (Fig 2b). When these larvae were assayed around the
253 pec-fin stage (60 hpf), pigmentation patterns in control conditions showed a fully pigmented RPE.

254 By contrast, injected larvae showed a pigmentation pattern in the form of patches of diminished
255 pigmentation (Fig 2b). Prior *mitfb* LoF studies have indicated that a combination of *mitfa, mitfb*
256 and the *otx* genes is necessary for proper development of the RPE in zebrafish[33]. Therefore,
257 silencing *mitfb* likely delays RPE pigmentation as a consequence of delaying its development.
258 Furthermore, individual *mitfb* sgRNAs, whether they targeted the promoter or 5'-UTR, were
259 capable of modulating *mitfb* expression and resulted in patches of reduced pigmentation in the
260 RPE (Supp Fig 3). However, the level of modulation induced by each sgRNA differed as some of
261 them presented with hypopigmented patches around the prim 20-25 stages (33-36 hpf) and their
262 effect was still noticeable at the pec-fin stage (60 hpf) (Supp Fig 3). By contrast, other sgRNAs
263 were able to modulate *mitfb* around the prim 20-25 stages (33-36 hpf) but their effect had
264 dissipated by the pec-fin stage (60 hpf) (Supp Fig 3), confirming the transient effect of our
265 CRISPRi system.

266 These results imply that our zebrafish codon-optimized CRISPRi is effective at modulating
267 expression of the *mitf* genes, which results in indirect modulation of *tyr* gene expression amongst
268 other genes, leading to melanocyte hypopigmentation.

269

270 **CRISPRi targeting of transcription factor *sox10* silences pigmentation pathway in**
271 **zebrafish**

272 Having established that *tyr*, and *mitfa/b* can be modulated via CRISPRi, we sought to
273 move our assays upstream of these factors, investigating whether *sox10*, a transcription factor
274 known to activate *mitfa/b* and to promote melanin production in zebrafish and other
275 vertebrates[35,36]. We designed sgRNAs to target the promoter of the *sox10* gene, predicting that
276 silencing it would lead to downregulation of *mitfa/b* and *tyr* and subsequent hypopigmentation in
277 the zebrafish.

278 Four gRNAs were designed to target the *sox10* promoter (Methods). Zebrafish larvae (n
279 ≥ 200) injected with CRISPRi (300 ng/µl) and a cocktail of all *sox10* sgRNAs (150 ng/each)

280 displayed marked reduction in pigmentation of melanocytes, assayed wihtin prim 20-25 (33-36
281 hpf), consistent with reduction of pigmentation when targeting downstream genes *mitfa/b,* and *tyr*
282 (Fig 3A, Supp Fig 4). Consistent with our results, no reduction in pigmentation was observed in
283 larvae receiving only the CRISPRi mRNA (n ≥ 200) or uninjected controls (n ≥ 200) (Fig 3A).
284 Furthermore, we observed that at least one sgRNAs (Fig 3A, 3B, Supp Fig 4) was effective at
285 reducing pigmentation when injected individually. These results are in line with previous work that
286 demonstrated that *sox10* is important for melanocyte development and melanin production[35,36,59].
287 The effects of CRISPRi dissipated by the pec-fin stage (60 hpf) as the pigmentation patterns
288 between injected and uninjected were indistinguishable (Fig 3A).

289 Because *sox10* also targets *mitfb* for activation, we investigated if silencing *sox10* would
290 have any effect on the RPE. We observed that silencing *sox10* leads to delay in pigmentation in
291 the RPE (Fig 3B). Consistent with our results, around the prim 20-25 stages (33-36 hpf), the RPE
292 is not fully pigmented, and no differences are observed between controls and experimental
293 conditions (Supp Fig 4). At the pec-fin stage (60 hpf), different pigmentation patterns in the form
294 of patches of hypopigmentation between conditions were observed ventrally in injected larvae
295 (Fig 3B). This is similar to the phenotype observed when targeting *mitfb*, suggesting that silencing
296 *sox10* leads to reduced transcription of *mitfb,* which leads to subsequent delay in RPE
297 development and pigmentation. By contrast, the RPE in controls was fully pigmented at the pec-
298 fin stage (60 hpf) (Fig 3B).

299 These results imply that our zebrafish codon-optimized CRISPRi is effective at modulating
300 the expression of any particular gene and the effect of silencing any gene leads to downregulation
301 of downstream genes.

302

303 **CRISPRi/a affects zebrafish length by modulating transcription of *mrap2a***

304 Considering the successful demonstration of CRISPRi-mediated modulation of zebrafish
305 pigmentation, we then set out to test our CRISPRa system focusing on growth, a potentially more

306 informative phenotype for this test. We targeted the *mrap2a* gene which is known to regulate the
307 expression of the melanocortin 4 receptor (*mc4r*) gene by silencing its transcription[50,60]. Both
308 genes have been shown to be involved in energy homeostasis and somatic growth in mice and
309 zebrafish and are thought to be heavily involved in familial early-onset obesity in humans[61].
310 Targeting *mrap2a* with CRISPRa and increasing its transcription would result in a decrease in
311 *mc4r* transcription, which would lead to an increase in larval length. By contrast, silencing *mrap2a*
312 with CRISPRi and decreasing its transcription would lead to an increase in *mc4r* expression,
313 resulting in larvae shorter in length[50,61].

314 While many loss-of-function experiments have been performed targeting *mrap2a*[50,60,61],
315 gain-of-function (GoF) experiments targeting *mrap2a* have not been explored. As a proof-of-
316 principle experiment, we designed four sgRNAs to target the *mrap2a* promoter (Methods) with
317 our CRISPRa system. Zebrafish larvae (n ≥ 200) injected with CRISPRa (300 ng/µl) and a cocktail
318 of all *mrap2a* sgRNAs (150 ng/each) displayed marked increase in body length, assayed at the
319 pec-fin stage (60 hpf) (Fig 4A). Similarly, we tested if an individual sgRNA could guide the dCas9-
320 VP64 to modulate body length and found sgRNA3 (150 ng) capable of inducing an observable
321 phenotype (Fig 4A, 4B). By contrast, no increase in larval length was observed at the pec-fin
322 stage (60 hpf) in larvae receiving only the CRISPRa mRNA (n ≥ 200) or in uninjected controls (n
323 ≥ 200). Moreover, the effects of CRISPRa were still noticeable at the day 5 stage (120 hpf) and
324 within the day 7-13 stage (>168 hpf), as the length of these larvae was still longer than control
325 conditions (Fig 4A, Supp Fig 5). Furthermore, we measured the length of larvae receiving
326 CRISPRa+sgRNA3 (n = 50), sgRNA3-only (n = 50), and uninjected controls (n = 50) and
327 performed a Welch two-sample t-test to analyze if the average length between these conditions
328 was statistically different (Fig 4B). At the pec-fin stage (60 hpf), the average length for these
329 conditions was 3673.67 µm, 3468.86 µm, and 3466.28 µm (p-value = 8.58e-16; 1.83e-14, and
330 0.9181), respectively. The longer larval length phenotype due to increased *mrap2a* transcription
331 and decreased *mc4r* expression is consistent with increased size and weight in mice that become

332 obese due to *mc4r* haploinsufficiency[29], and with morbid obesity cases in humans due to
333 frameshift (loss of function) mutations in *mc4r*[62].

334 We used the same sgRNAs to target and silence *mrap2a* and increase *mc4r* expression.
335 Zebrafish larvae (n ≥ 200) injected with CRISPRi (300 ng/µl) plus all sgRNAs (150 ng/µl/each)
336 displayed a decrease in larval length at the pec-fin stage (60 hpf) (Fig 4A, 4C), which is consistent
337 with rescuing obese mice with *mc4r* haploinsufficiency[29]. Additionally, sgRNA3 was able to guide
338 the dCas9-KRAB-MeCP2 to modulate silencing of *mrap2a* individually and led to a decrease in
339 larval length, observed at the pec-fin stage (60 hpf) (Fig 4A. 4C). By contrast, larval length
340 observed at the pec-fin stage (60 hpf) for larvae receiving only the CRISPRi mRNA (n ≥ 200) or
341 in uninjected controls (n ≥ 200) was higher than our experimental condition (Fig 4A). Further,
342 larvae injected with CRISPRi still displayed a shorter length around the day 5 stage (120 hpf), but
343 their length was similar to controls within day 7-13 (>168 hpf) (Fig 4A, Supp Fig 5). We also
344 measured the larval length for the conditions CRISPRi+sgRNA3 (n = 50), sgRNA3-only (n = 50),
345 and uninjected controls (n = 50) and found their average length to be 3481.98 µm, 3779.96 µm,
346 and 3748.82 µm, respectively (Fig 4B). We analyzed the statistical significance between these
347 means with a Welch two-sample t-test and found the difference in means between experimental
348 and control conditions to be statistically significant (p-values = 2.2e-16, 2.2e-16, and 0.0636). This
349 further demonstrates that modulating the regulation of one can elicit indirect regulation of other
350 target genes, opening the door to a better understanding of gene regulatory networks and their
351 exploration for potential therapeutic interventions.
352

353 DISCUSSION
354

355 CRISPRi/a has emerged as a powerful tool in genetic research, offering the ability to
356 modulate gene expression both for exploration of fundamental mechanisms and for potential

357 therapeutics. It offers the capacity to modulate gene expression without inducing genetic
358 alterations which makes CRISPRi/a avaluable technology for the study of gene regulation and for
359 efficient exploration of both gain and loss of function phenotypes. Nevertheless, its development
360 and application in zebrafish has been slow over the past decade, with only one study describing
361 an effort to implement it[26]., while many others apply CRISPR-based editing
362 technologies[18,19,21,53,54,63].

363 In this study, we chose to fuse a catalytically inactive Cas9 with the transcriptional
364 repressor KRAB-MeCP2. Our choice to use dCas9-KRAB-MeCP2 was guided by previous
365 studies that demonstrated its ability to induce gene silencing while outperforming dCas9-KRAB
366 systems[24,64], implemented in previous CRISPRi experiments in zebrafish[26]. In contrast, for our
367 CRISPRa system, we fused the dCas9 with the transcriptional activator VP64. Comparisons
368 between different Cas9 activators have demonstrated the VP64 to effectively induce gene
369 activation[25]. And while other Cas9 activators such as VPR, SAM, and Suntag have been shown
370 to outperform VP64, these systems have not been tested in zebrafish and/or require special
371 sgRNAs to induce their effect. By using a catalytically inactive Cas9 fused with the transcriptional
372 repressors KRAB-MeCP2 or the transcriptional activator VP64, we have achieved transcriptional
373 control over key genes involved in melanocyte differentiation (*sox10, mitfa, mitfb*), pigmentation
374 (*tyr*), and somatic growth (*mrap2a*) in zebrafish. Our results underscore the versatility and
375 efficiency of CRISPRi/a in zebrafish research. For instance, by silencing *sox10, mitfa, mitfb*, and
376 *tyr*, we successfully were able to obtain zebrafish larvae with marked reduction in pigmentation.
377 Similarly, by activating or silencing *mrap2a*, we successfully modulated larval length.

378 These proof-of-principle experiments underscore the potential of CRISPRi/a technology
379 to control gene expression by targeting gene promoters. CRISIPRi/a is relatively straightforward
380 to implement compared to other genetic editing technologies, which further increases its appeal.
381 In addition, implementing this technology in transparent one-cell zebrafish embryos makes it
382 easier to study the effects of gene silencing and activation during development. Further,

383 CRISPRi/a can also be implemented to study the effects of silencing or activating noncoding
384 regulatory sequences such as enhancers, repressors, and insulators. Taking advantage of the
385 fact that approximately 70% of human genes have a zebrafish gene homolog facilitates the study
386 of gene regulatory mechanisms and networks in yet another vertebrate system. The versatility to
387 study gene expression modulation by either targeting gene promoters or any potential noncoding
388 regulatory sequences in a vertebrate system can offer insights into disease pathogenesis and
389 therapeutic targets that may translate to clinical applications.

390 CRISPRi/a technology, just like CRISPR gene editing, can also be limited by off-target
391 effects and variability in efficiency across genomic loci. Additionally, the ethical implications of
392 gene expression modulation and the potential for unintended consequences underscore the
393 importance of careful consideration in the application of this technology. In this current study, the
394 primary limitation is the delivery of CRISPRi/a via mRNA microinjections, which is titrated as the
395 embryo develops and the larvae grow older. This results in a diminution of an observable
396 phenotype and hinders the potential to study long-term effects of gene expression modulation,
397 making it difficult to elucidate any potential disease relevance. To this end, we are actively
398 generating stable transgenic lines expressing CRISPRi/a to facilitate rapid and systematic
399 screening of gain or loss of gene function. Our ongoing work will expand the zebrafish toolkit,
400 establishing the utility of CRISPRi/a for evaluation of candidate gene function and disease
401 relevance.

402

403 AUTHOR CONTRIBUTIONS: A.S.M., V.C.C, and N.B.B. conceptualized the study. N.B.B.
404 designed codon optimized dCas9-KRAB-MeCP2 and dCas9-VP64 constructs and custom single
405 guide RNAs. N.B.B., E.A.S., and R.J.B. injected RNA constructs into zebrafish embryos. N.B.B.
406 and E.A.S. imaged the fish. N.B.B. and R.J.B. wrote the manuscript. All authors edited and
407 approved the final manuscript for publication.

408

FUNDING: This research, undertaken at Johns Hopkins University School of Medicine, was supported in part by awards from the National Institutes of Health to A.S.M. (R01HG010480 and R21NS128604), V.C.C. (R35 GM136644), as well as N.B.B., E.A.S., and R.J.B. (T32 GM007814-40); and by the Canadian Institutes of Health Research (DFD-181599) to R.J.B.

DATA AVAILABILITY: N/A

ACKNOWLEDGEMENTS: The authors would like to acknowledge the FInZ Zebrafish Core Center for assistance with zebrafish husbandry.

CONFLICTS OF INTEREST: The authors declare no competing interests.

425 REFERENCES

426

427 1. Giffen, K.P., Liu, H., Kramer, K.L., and He, D.Z. (2019). Expression of Protein-Coding Gene
428 Orthologs in Zebrafish and Mouse Inner Ear Non-sensory Supporting Cells. Front Neurosci
429 *13*. https://doi.org/10.3389/FNINS.2019.01117/FULL.

430 2. Howe, K., Clark, M.D., Torroja, C.F., Torrance, J., Berthelot, C., Muffato, M., Collins, J.E.,
431 Humphray, S., McLaren, K., Matthews, L., et al. (2013). The zebrafish reference genome
432 sequence and its relationship to the human genome. Nature *496*, 498–503.
433 https://doi.org/10.1038/NATURE12111.

434 3. Fisher, S., Grice, E.A., Vinton, R.M., Bessling, S.L., Urasaki, A., Kawakami, K., and McCallion,
435 A.S. (2006). Evaluating the biological relevance of putative enhancers using Tol2
436 transposon-mediated transgenesis in zebrafish. Nature Protocols 2006 1:3 *1*, 1297–1305.
437 https://doi.org/10.1038/nprot.2006.230.

438 4. Gorkin, D.U., Lee, D., Reed, X., Fletez-Brant, C., Bessling, S.L., Loftus, S.K., Beer, M.A.,
439 Pavan, W.J., and McCallion, A.S. (2012). Integration of ChIP-seq and machine learning
440 reveals enhancers and a predictive regulatory sequence vocabulary in melanocytes.
441 Genome Res *22*, 2290–2301. https://doi.org/10.1101/GR.139360.112.

442 5. Fisher, S., Grice, E.A., Vinton, R.M., Bessling, S.L., and McCallion, A.S. (2006). Conservation
443 of RET regulatory function from human to zebrafish without sequence similarity. Science
444 *312*, 276–279. https://doi.org/10.1126/SCIENCE.1124070.

445 6. Antonellis, A., Huynh, J.L., Lee-Lin, S.Q., Vinton, R.M., Renaud, G., Loftus, S.K., Elliot, G.,
446 Wolfsberg, T.G., Green, E.D., McCallion, A.S., et al. (2008). Identification of neural crest and
447 glial enhancers at the mouse Sox10 locus through transgenesis in zebrafish. PLoS Genet *4*.
448 https://doi.org/10.1371/JOURNAL.PGEN.1000174.

449 7. Doyle, A.J., Doyle, J.J., Bessling, S.L., Maragh, S., Lindsay, M.E., Schepers, D., Gillis, E.,
450 Mortier, G., Homfray, T., Sauls, K., et al. (2012). Mutations in the TGF-β repressor SKI cause
451 Shprintzen-Goldberg syndrome with aortic aneurysm. Nat Genet *44*, 1249–1254.
452 https://doi.org/10.1038/NG.2421.

453 8. Gould, R.A., Aziz, H., Woods, C.E., Seman-Senderos, M.A., Sparks, E., Preuss, C.,
454 Wünnemann, F., Bedja, D., Moats, C.R., McClymont, S.A., et al. (2019). ROBO4 variants
455 predispose individuals to bicuspid aortic valve and thoracic aortic aneurysm. Nat Genet *51*,
456 42–50. https://doi.org/10.1038/S41588-018-0265-Y.

457 9. Golzio, C., Willer, J., Talkowski, M.E., Oh, E.C., Taniguchi, Y., Jacquemont, S., Reymond, A.,
458 Sun, M., Sawa, A., Gusella, J.F., et al. (2012). KCTD13 is a major driver of mirrored
459 neuroanatomical phenotypes of the 16p11.2 copy number variant. Nature *485*, 363–367.
460 https://doi.org/10.1038/NATURE11091.

461 10. Panizzi, J.R., Becker-Heck, A., Castleman, V.H., Al-Mutairi, D.A., Liu, Y., Loges, N.T., Pathak,
462 N., Austin-Tse, C., Sheridan, E., Schmidts, M., et al. (2012). CCDC103 mutations cause

463 primary ciliary dyskinesia by disrupting assembly of ciliary dynein arms. Nat Genet *44*, 714–
464 719. https://doi.org/10.1038/NG.2277.

465 11. Roscioli, T., Kamsteeg, E.J., Buysse, K., Maystadt, I., Van Reeuwijk, J., Van Den Elzen, C., Van
466 Beusekom, E., Riemersma, M., Pfundt, R., Vissers, L.E.L.M., et al. (2012). Mutations in ISPD
467 cause Walker-Warburg syndrome and defective glycosylation of α-dystroglycan. Nat Genet
468 *44*, 581–585. https://doi.org/10.1038/NG.2253.

469 12. Tobin, D.M., Roca, F.J., Oh, S.F., McFarland, R., Vickery, T.W., Ray, J.P., Ko, D.C., Zou, Y.,
470 Bang, N.D., Chau, T.T.H., et al. (2012). Host genotype-specific therapies can optimize the
471 inflammatory response to mycobacterial infections. Cell *148*, 434–446.
472 https://doi.org/10.1016/J.CELL.2011.12.023.

473 13. Maragh, S., Miller, R.A., Bessling, S.L., McGaughey, D.M., Wessels, M.W., De Graaf, B.,
474 Stone, E.A., Bertoli-Avella, A.M., Gearhart, J.D., Fisher, S., et al. (2011). Identification of RNA
475 binding motif proteins essential for cardiovascular development. BMC Dev Biol *11*.
476 https://doi.org/10.1186/1471-213X-11-62.

477 14. Wahbeh, M.H., Boyd, R.J., Yovo, C., Rike, B., McCallion, A.S., and Avramopoulos, D. (2024).
478 A functional schizophrenia-associated genetic variant near the TSNARE1 and ADGRB1
479 genes. HGG Adv *5*. https://doi.org/10.1016/J.XHGG.2024.100303.

480 15. Asakawa, K., and Kawakami, K. (2008). Targeted gene expression by the Gal4-UAS system in
481 zebrafish. Dev Growth Differ *50*, 391–399. https://doi.org/10.1111/J.1440-
482 169X.2008.01044.X.

483 16. Zhu, C., Smith, T., Mcnulty, J., Rayla, A.L., Lakshmanan, A., Siekmann, A.F., Buffardi, M.,
484 Meng, X., Shin, J., Padmanabhan, A., et al. (2011). Evaluation and application of modularly
485 assembled zinc-finger nucleases in zebrafish. Development *138*, 4555–4564.
486 https://doi.org/10.1242/DEV.066779.

487 17. Huang, P., Xiao, A., Zhou, M., Zhu, Z., Lin, S., and Zhang, B. (2011). Heritable gene targeting
488 in zebrafish using customized TALENs. Nature Biotechnology 2011 29:8 *29*, 699–700.
489 https://doi.org/10.1038/nbt.1939.

490 18. Hwang, W.Y., Fu, Y., Reyon, D., Maeder, M.L., Tsai, S.Q., Sander, J.D., Peterson, R.T., Yeh,
491 J.R.J., and Joung, J.K. (2013). Efficient genome editing in zebrafish using a CRISPR-Cas
492 system. Nat Biotechnol *31*, 227–229. https://doi.org/10.1038/NBT.2501.

493 19. Shah, A.N., Davey, C.F., Whitebirch, A.C., Miller, A.C., and Moens, C.B. (2015). Rapid
494 reverse genetic screening using CRISPR in zebrafish. Nat Methods *12*, 535–540.
495 https://doi.org/10.1038/NMETH.3360.

496 20. Varshney, G.K., Pei, W., Lafave, M.C., Idol, J., Xu, L., Gallardo, V., Carrington, B., Bishop, K.,
497 Jones, M., Li, M., et al. (2015). High-throughput gene targeting and phenotyping in zebrafish
498 using CRISPR/Cas9. Genome Res *25*, 1030–1042. https://doi.org/10.1101/GR.186379.114.

499 21. Zhang, Y., Qin, W., Lu, X., Xu, J., Huang, H., Bai, H., Li, S., and Lin, S. (2017). Programmable
500 base editing of zebrafish genome using a modified CRISPR-Cas9 system. Nat Commun *8*.
501 https://doi.org/10.1038/S41467-017-00175-6.

502 22. Hisano, Y., Sakuma, T., Nakade, S., Ohga, R., Ota, S., Okamoto, H., Yamamoto, T., and
503 Kawahara, A. (2015). Precise in-frame integration of exogenous DNA mediated by
504 CRISPR/Cas9 system in zebrafish. Sci Rep *5*. https://doi.org/10.1038/SREP08841.

505 23. Larson, M.H., Gilbert, L.A., Wang, X., Lim, W.A., Weissman, J.S., and Qi, L.S. (2013). CRISPR
506 interference (CRISPRi) for sequence-specific control of gene expression. Nature Protocols
507 2013 8:11 *8*, 2180–2196. https://doi.org/10.1038/nprot.2013.132.

508 24. Yeo, N.C., Chavez, A., Lance-Byrne, A., Chan, Y., Menn, D., Milanova, D., Kuo, C.C., Guo, X.,
509 Sharma, S., Tung, A., et al. (2018). An enhanced CRISPR repressor for targeted mammalian
510 gene regulation. Nat Methods *15*, 611–616. https://doi.org/10.1038/S41592-018-0048-5.

511 25. Chavez, A., Tuttle, M., Pruitt, B.W., Ewen-Campen, B., Chari, R., Ter-Ovanesyan, D., Haque,
512 S.J., Cecchi, R.J., Kowal, E.J.K., Buchthal, J., et al. (2016). Comparison of Cas9 activators in
513 multiple species. Nat Methods *13*, 563–567. https://doi.org/10.1038/NMETH.3871.

514 26. Long, L., Guo, H., Yao, D., Xiong, K., Li, Y., Liu, P., Zhu, Z., and Liu, D. (2015). Regulation of
515 transcriptionally active genes via the catalytically inactive Cas9 in C. elegans and D. rerio.
516 Cell Research 2015 25:5 *25*, 638–641. https://doi.org/10.1038/cr.2015.35.

517 27. Sastre, D., Zafar, F., Torres, C.A.M., Piper, D., Kirik, D., Sanders, L.H., Qi, L.S., and Schüle, B.
518 (2023). Inactive S. aureus Cas9 downregulates alpha-synuclein and reduces mtDNA
519 damage and oxidative stress levels in human stem cell model of Parkinson's disease. Sci
520 Rep *13*. https://doi.org/10.1038/S41598-023-45078-3.

521 28. Matharu, N., and Ahituv, N. (2020). Modulating gene regulation to treat genetic disorders.
522 Nature Reviews Drug Discovery 2020 19:11 *19*, 757–775. https://doi.org/10.1038/s41573-
523 020-0083-7.

524 29. Matharu, N., Rattanasopha, S., Tamura, S., Maliskova, L., Wang, Y., Bernard, A., Hardin, A.,
525 Eckalbar, W.L., Vaisse, C., and Ahituv, N. (2019). CRISPR-mediated activation of a promoter
526 or enhancer rescues obesity caused by haploinsufficiency. Science (1979) *363*.
527 https://doi.org/10.1126/SCIENCE.AAU0629/SUPPL_FILE/AAU0629_TABLE_S6.XLSX.

528 30. Camp, E., and Lardelli, M. (2001). Tyrosinase gene expression in zebrafish embryos. Dev
529 Genes Evol *211*, 150–153. https://doi.org/10.1007/S004270000125/METRICS.

530 31. Cooper, C.D., and Raible, D.W. (2009). Mechanisms for reaching the differentiated state:
531 Insights from neural crest-derived melanocytes. Semin Cell Dev Biol *20*, 105–110.
532 https://doi.org/10.1016/J.SEMCDB.2008.09.008.

533 32. Haffter, P., Odenthal, J., Mullins, M.C., Lin, S., Farrell, M.J., Vogelsang, E., Haas, F., Brand,
534 M., Van Eeden, F.J.M., Furutani-Seiki, M., et al. (1996). Mutations affecting pigmentation and
535 shape of the adult zebrafish. Dev Genes Evol *206*, 260–276.
536 https://doi.org/10.1007/S004270050051/METRICS.

537 33. Lane, B.M., and Lister, J.A. (2012). Otx but Not Mitf Transcription Factors Are Required for
538 Zebrafish Retinal Pigment Epithelium Development. PLoS One *7*, 49357.
539 https://doi.org/10.1371/JOURNAL.PONE.0049357.

540 34. Lister, J.A., Close, J., and Raible, D.W. (2001). Duplicate mitf genes in zebrafish:
541 complementary expression and conservation of melanogenic potential. Dev Biol *237*, 333–
542 344. https://doi.org/10.1006/DBIO.2001.0379.

543 35. Murisier, F., Guichard, S., and Beermann, F. (2007). The tyrosinase enhancer is activated by
544 Sox10 and Mitf in mouse melanocytes. Pigment Cell Res *20*, 173–184.
545 https://doi.org/10.1111/J.1600-0749.2007.00368.X.

546 36. Dutton, K.A., Pauliny, A., Lopes, S.S., Elworthy, S., Carney, T.J., Rauch, J., Geisler, R.,
547 Haffter, P., and Kelsh, R.N. (2001). Zebrafish colourless encodes sox10 and specifies non-
548 ectomesenchymal neural crest fates. Development *128*, 4113–4125.
549 https://doi.org/10.1242/DEV.128.21.4113.

550 37. Johnson, S.L., Nguyen, A.T.N., and Lister, J.A. (2011). mitfa is required at multiple stages of
551 melanocyte differentiation but not to establish the melanocyte stem cell. Dev Biol *350*, 405.
552 https://doi.org/10.1016/J.YDBIO.2010.12.004.

553 38. Wang, C., Kocher, T.D., Wu, J., Li, P., Liang, G., Lu, B., Xu, J., Chen, X., and Wang, D. (2023).
554 Knockout of microphthalmia-associated transcription factor (mitf) confers a red and yellow
555 tilapia with few pigmented melanophores. Aquaculture *565*, 739151.
556 https://doi.org/10.1016/J.AQUACULTURE.2022.739151.

557 39. Wu, Y.C., and Wang, I.J. (2020). Heat-shock-induced tyrosinase gene ablation with CRISPR
558 in zebrafish. Molecular Genetics and Genomics *295*, 911–922.
559 https://doi.org/10.1007/S00438-020-01681-X/FIGURES/6.

560 40. Camp, E., Badhwar, P., Mann, G.J., and Lardelli, M. (2003). Expression Analysis of a
561 Tyrosinase Promoter Sequence in Zebrafish. Pigment Cell Res *16*, 117–126.
562 https://doi.org/10.1034/J.1600-0749.2003.00002.X.

563 41. Frantz, W.T., and Ceol, C.J. (2020). From Tank to Treatment: Modeling Melanoma in
564 Zebrafish. Cells *9*. https://doi.org/10.3390/CELLS9051289.

565 42. Praetorius, C., Grill, C., Stacey, S.N., Metcalf, A.M., Gorkin, D.U., Robinson, K.C., Van
566 Otterloo, E., Kim, R.S.Q., Bergsteinsdottir, K., Ogmundsdottir, M.H., et al. (2013). A
567 polymorphism in IRF4 affects human pigmentation through a tyrosinase-dependent
568 MITF/TFAP2A pathway. Cell *155*, 1022. https://doi.org/10.1016/J.CELL.2013.10.022.

569 43. Rosenbaum, S.R., Tiago, M., Caksa, S., Capparelli, C., Purwin, T.J., Kumar, G., Glasheen, M.,
570 Pomante, D., Kotas, D., Chervoneva, I., et al. (2021). SOX10 requirement for melanoma
571 tumor growth is due, in part, to immune-mediated effects. Cell Rep *37*.
572 https://doi.org/10.1016/J.CELREP.2021.110085.

573 44. Gudbjartsson, D.F., Sulem, P., Stacey, S.N., Goldstein, A.M., Rafnar, T., Sigurgeirsson, B.,
574 Benediktsdottir, K.R., Thorisdottir, K., Ragnarsson, R., Sveinsdottir, S.G., et al. (2008). ASIP

575 and TYR pigmentation variants associate with cutaneous melanoma and basal cell
576 carcinoma. Nat Genet *40*, 886–891. https://doi.org/10.1038/NG.161.

577 45. Garraway, L.A., Widlund, H.R., Rubin, M.A., Getz, G., Berger, A.J., Ramaswamy, S.,
578 Beroukhim, R., Milner, D.A., Granter, S.R., Du, J., et al. (2005). Integrative genomic analyses
579 identify MITF as a lineage survival oncogene amplified in malignant melanoma. Nature *436*,
580 117–122. https://doi.org/10.1038/NATURE03664.

581 46. Tassabehji, M., Newton, V.E., and Read, A.P. (1994). Waardenburg syndrome type 2 caused
582 by mutations in the human microphthalmia (MITF) gene. Nat Genet *8*, 251–255.
583 https://doi.org/10.1038/NG1194-251.

584 47. Bondurand, N., Pingault, V., Goerich, D.E., Lemort, N., Sock, E., Le Caignec, C., Wegner, M.,
585 and Goossens, M. (2000). Interaction among SOX10, PAX3 and MITF, three genes altered in
586 Waardenburg syndrome. Hum Mol Genet *9*, 1907–1917.
587 https://doi.org/10.1093/HMG/9.13.1907.

588 48. Paratore, C., Eichenberger, C., Suter, U., and Sommer, L. (2002). Sox10 haploinsufficiency
589 affects maintenance of progenitor cells in a mouse model of Hirschsprung disease. Hum
590 Mol Genet *11*, 3075–3085. https://doi.org/10.1093/HMG/11.24.3075.

591 49. Mccallion, A.S., and Chakravarti, A. (2001). EDNRB/EDN3 and Hirschsprung disease type II.
592 Pigment Cell Res *14*, 161–169. https://doi.org/10.1034/J.1600-0749.2001.140305.X.

593 50. Sebag, J.A., Zhang, C., Hinkle, P.M., Bradshaw, A.M., and Cone, R.D. (2013). Developmental
594 Control of the Melanocortin-4 Receptor by MRAP2 Proteins in Zebrafish. Science *341*, 278.
595 https://doi.org/10.1126/SCIENCE.1232995.

596 51. Yeo, G.S.H., Farooqi, I.S., Aminian, S., Halsall, D.J., Stanhope, R.G., and O'Rahilly, S. (1998).
597 A frameshift mutation in MC4R associated with dominantly inherited human obesity. Nat
598 Genet *20*, 111–112. https://doi.org/10.1038/2404.

599 52. Wade, K.H., Lam, B.Y.H., Melvin, A., Pan, W., Corbin, L.J., Hughes, D.A., Rainbow, K., Chen,
600 J.H., Duckett, K., Liu, X., et al. (2021). Loss-of-function mutations in the melanocortin 4
601 receptor in a UK birth cohort. Nat Med *27*, 1088–1096. https://doi.org/10.1038/S41591-021-
602 01349-Y.

603 53. Amorim, J.P., Bordeira-Carriço, R., Gali-Macedo, A., Perrod, C., and Bessa, J. (2020).
604 CRISPR-Cas9-Mediated Genomic Deletions Protocol in Zebrafish. STAR Protoc *1*.
605 https://doi.org/10.1016/J.XPRO.2020.100208.

606 54. Jao, L.E., Wente, S.R., and Chen, W. (2013). Efficient multiplex biallelic zebrafish genome
607 editing using a CRISPR nuclease system. Proc Natl Acad Sci U S A *110*, 13904–13909.
608 https://doi.org/10.1073/PNAS.1308335110.

609 55. Kimmel, C.B., Ballard, W.W., Kimmel, S.R., Ullmann, B., and Schilling, T.F. (1995). Stages of
610 embryonic development of the zebrafish. Developmental Dynamics *203*, 253–310.
611 https://doi.org/10.1002/aja.1002030302.

612 56. Kawakami, A., and Fisher, D.E. (2017). The master role of microphthalmia-associated
613 transcription factor in melanocyte and melanoma biology. Laboratory Investigation 2017
614 97:6 *97*, 649–656. https://doi.org/10.1038/labinvest.2017.9.

615 57. Cooper, C.D. (2017). Insights from zebrafish on human pigment cell disease and treatment.
616 Developmental Dynamics *246*, 889–896. https://doi.org/10.1002/DVDY.24550.

617 58. Moreno-Marmol, T., Cavodeassi, F., and Bovolenta, P. (2018). Setting eyes on the retinal
618 pigment epithelium. Front Cell Dev Biol *6*, 418922.
619 https://doi.org/10.3389/FCELL.2018.00145/BIBTEX.

620 59. Cunningham, R.L., Kramer, E.T., DeGeorgia, S.K., Godoy, P.M., Zarov, A.P., Seneviratne, S.,
621 Grigura, V., and Kaufman, C.K. (2021). Functional in vivo characterization of sox10
622 enhancers in neural crest and melanoma development. Communications Biology 2021 4:1
623 *4*, 1–15. https://doi.org/10.1038/s42003-021-02211-0.

624 60. Baron, M., Maillet, J., Huyvaert, M., Dechaume, A., Boutry, R., Loiselle, H., Durand, E.,
625 Toussaint, B., Vaillant, E., Philippe, J., et al. (2019). Loss-of-function mutations in MRAP2 are
626 pathogenic in hyperphagic obesity with hyperglycemia and hypertension. Nature Medicine
627 2019 25:11 *25*, 1733–1738. https://doi.org/10.1038/s41591-019-0622-0.

628 61. Asai, M., Ramachandrappa, S., Joachim, M., Shen, Y., Zhang, R., Nuthalapati, N.,
629 Ramanathan, V., Strochlic, D.E., Ferket, P., Linhart, K., et al. (2013). Loss of function of the
630 melanocortin 2 receptor accessory protein 2 is associated with mammalian obesity.
631 Science (1979) *341*, 275–278. https://doi.org/10.1126/SCIENCE.1233000/SUPPL_FILE/ASAI-
632 SM.PDF.

633 62. Vaisse, C., Clement, K., Durand, E., Hercberg, S., Guy-Grand, B., and Froguel, P. (2000).
634 Melanocortin-4 receptor mutations are a frequent and heterogeneous cause of morbid
635 obesity. J Clin Invest *106*, 253–262. https://doi.org/10.1172/JCI9238.

636 63. de Vrieze, E., de Bruijn, S.E., Reurink, J., Broekman, S., van de Riet, V., Aben, M., Kremer, H.,
637 and van Wijk, E. (2021). Efficient generation of knock-in zebrafish models for inherited
638 disorders using crispr-cas9 ribonucleoprotein complexes. Int J Mol Sci *22*, 9429.
639 https://doi.org/10.3390/IJMS22179429/S1.

640 64. Alerasool, N., Segal, D., Lee, H., and Taipale, M. (2020). An efficient KRAB domain for
641 CRISPRi applications in human cells. Nature Methods 2020 17:11 *17*, 1093–1096.
642 https://doi.org/10.1038/s41592-020-0966-x.

643

644

645

646 FIGURES

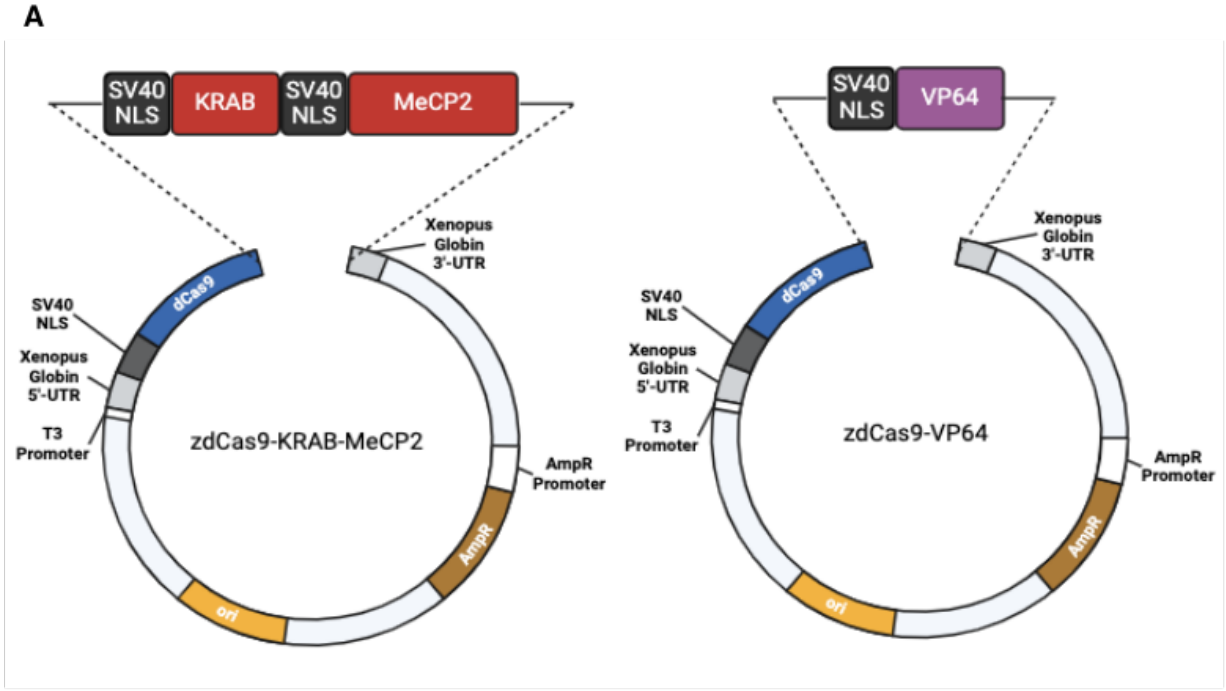

647

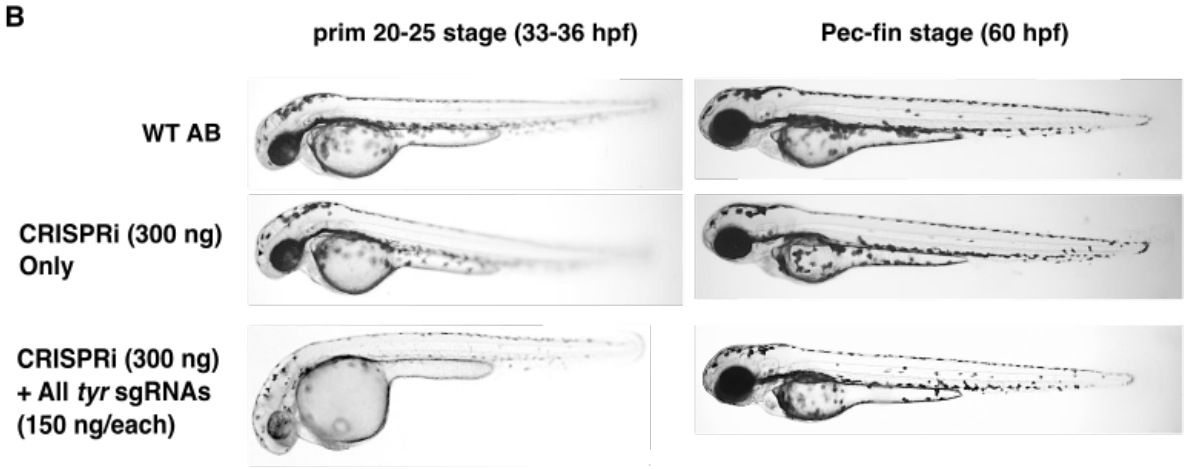

648

649 ***Figure 1:*** CRISPRi/a construct design. **A.** Zebrafish codon-optimized plasmids were linearized and *in vitro*
650 transcribed before microinjection into one-cell embryos. **B.** Zebrafish embryos injected with CRISPRi +
651 sgRNAs targeting *tyr* assayed at prim 20-25 and pec-fin stages for differences in pigmentation patterns.
652 The larvae injected with CRISPRi and sgRNAs displayed reduced pigmentation at prim 20-25 stage when
653 compared to controls. The effect of CRISPRi dissipated by the pec-find stage as observable pigmentation
654 patterns were indistinguishable.

655

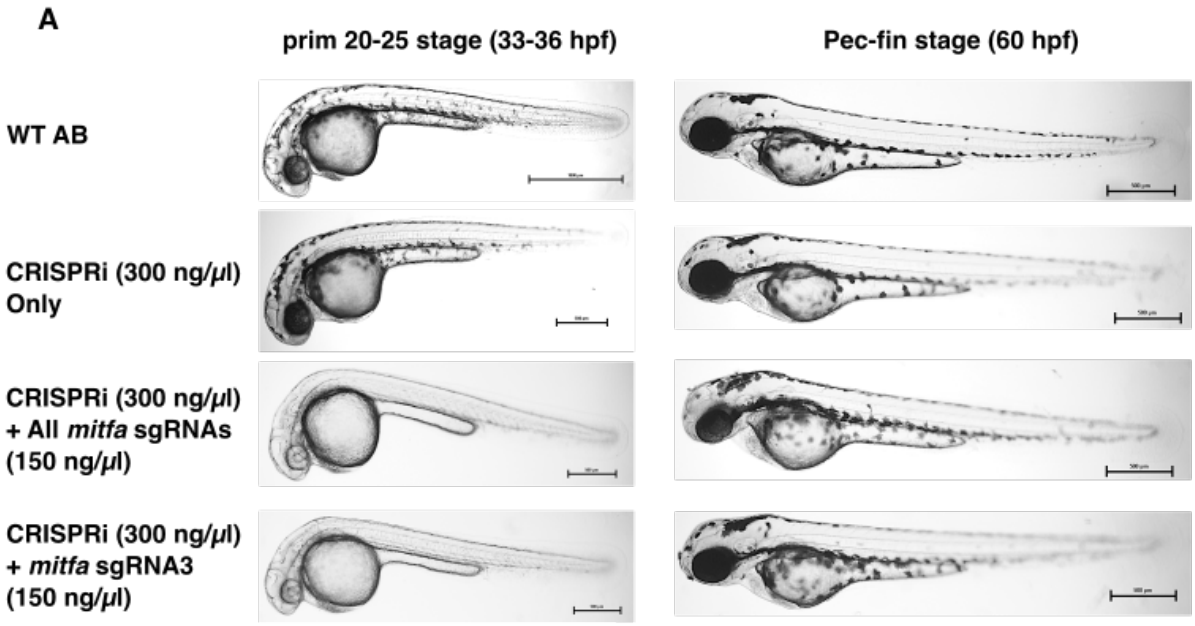

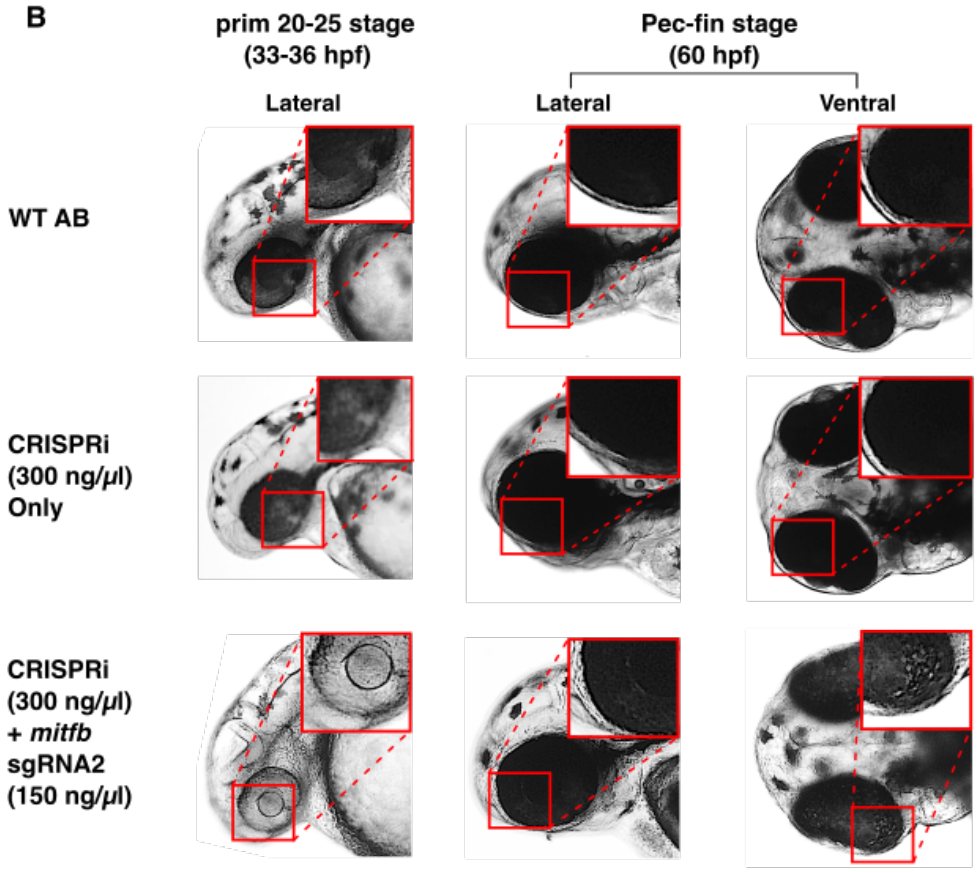

Figure 2: CRISPRi targeting the promoter of the *mitf* genes. **A.** Zebrafish embryos injected with CRISPRi + sgRNAs targeting *mitfa* assayed between prim 20 and pec-fin stages for differences in pigmentation patterns. WT AB and injected controls did not show reduced pigmentation around the prim 20-25 stages,

661 whereas embryos injected with all sgRNAs or only sgRNA3 displayed the hypopigmentation phenotype
662 around the prim 20-25 stages. The effect of CRISPRi dissipated by the pec-fin stage as patterns of
663 hypopigmentation were not observed between conditions. Scale bars: 500 or 1000 μm. **B.** Zebrafish
664 embryos injected with CRISPRi + sgRNAs targeting *mitfb* assayed between prim 20 and pec-fin stages for
665 differences in pigmentation patterns in the RPE. Among conditions, the RPE was not fully pigmented at
666 around the prim 20-25 stages. At the pec-fin stage, the RPE was fully pigmented among controls but not in
667 the experimental condition as seen laterally and ventrally.

668

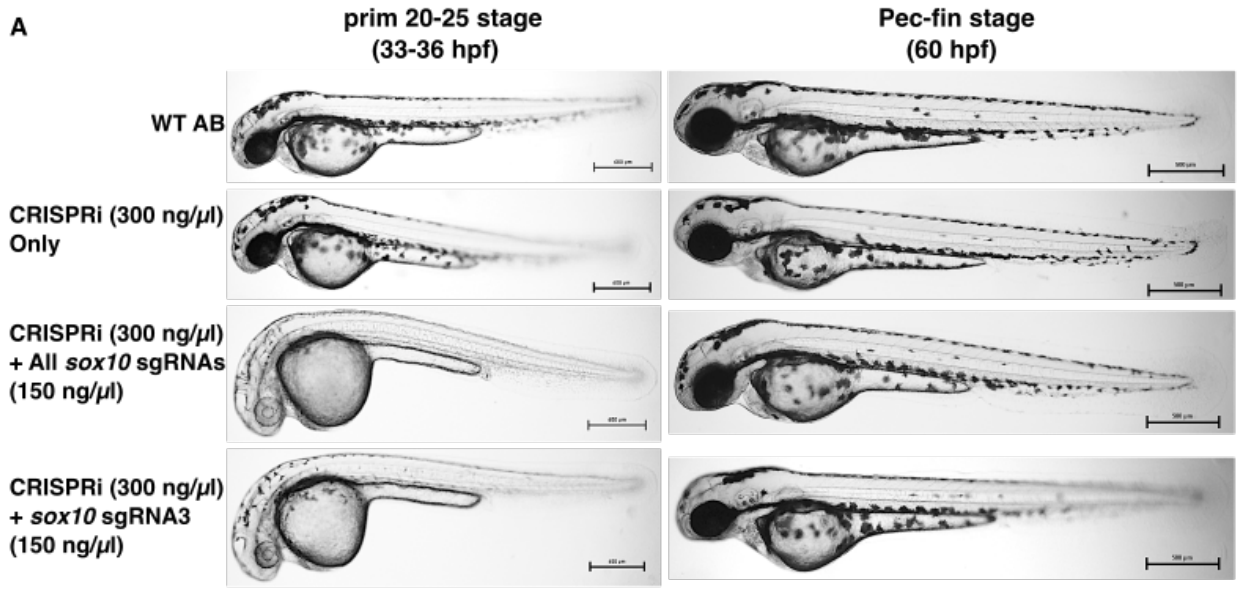

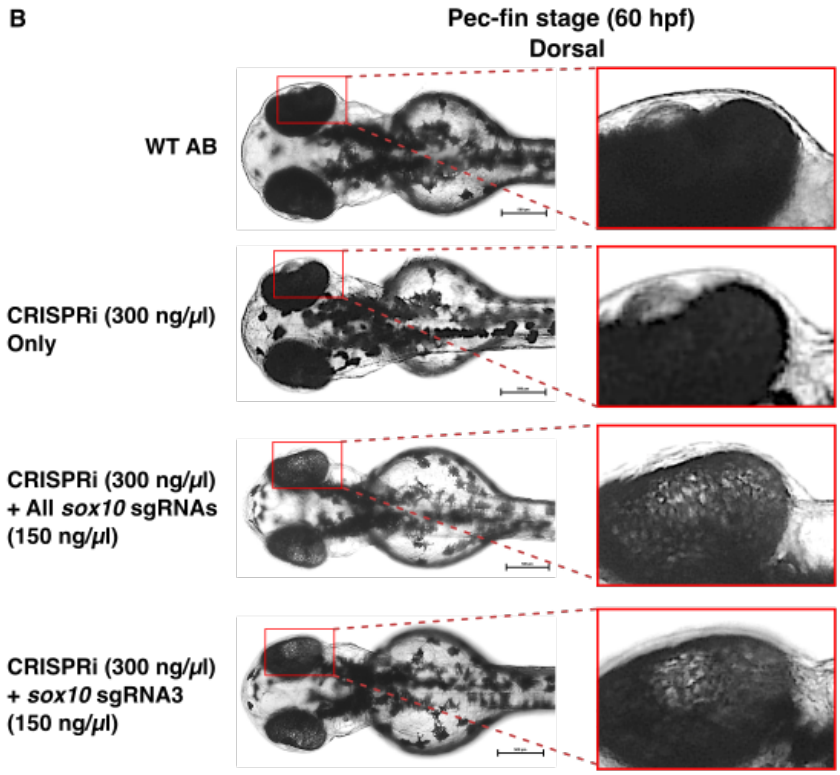

Figure 3: CRISPRi targeting the promoter of the *sox10* gene. **A.** Zebrafish embryos injected with CRISPRi + sgRNAs targeting *sox10* assayed between prim 20 and pec-fin stages for differences in pigmentation patterns. WT AB and injected controls did not show reduced pigmentation around the prim 20-25 stages, whereas embryos injected with CRISPRi + all sgRNAs or only sgRNA3 were hypopigmented and delayed in development (prim 20 stage). The effect of CRISPRi dissipated by the pec-fin stage as patterns of hypopigmentation were not observed between conditions. Scale bars: 600 µm. **B.** Silencing *sox10* creates patches of hypopigmentation in the RPE at the pec-fin stage. The RPE in controls is fully pigmented at the pec-fin stage. Scale bars 600 µm.

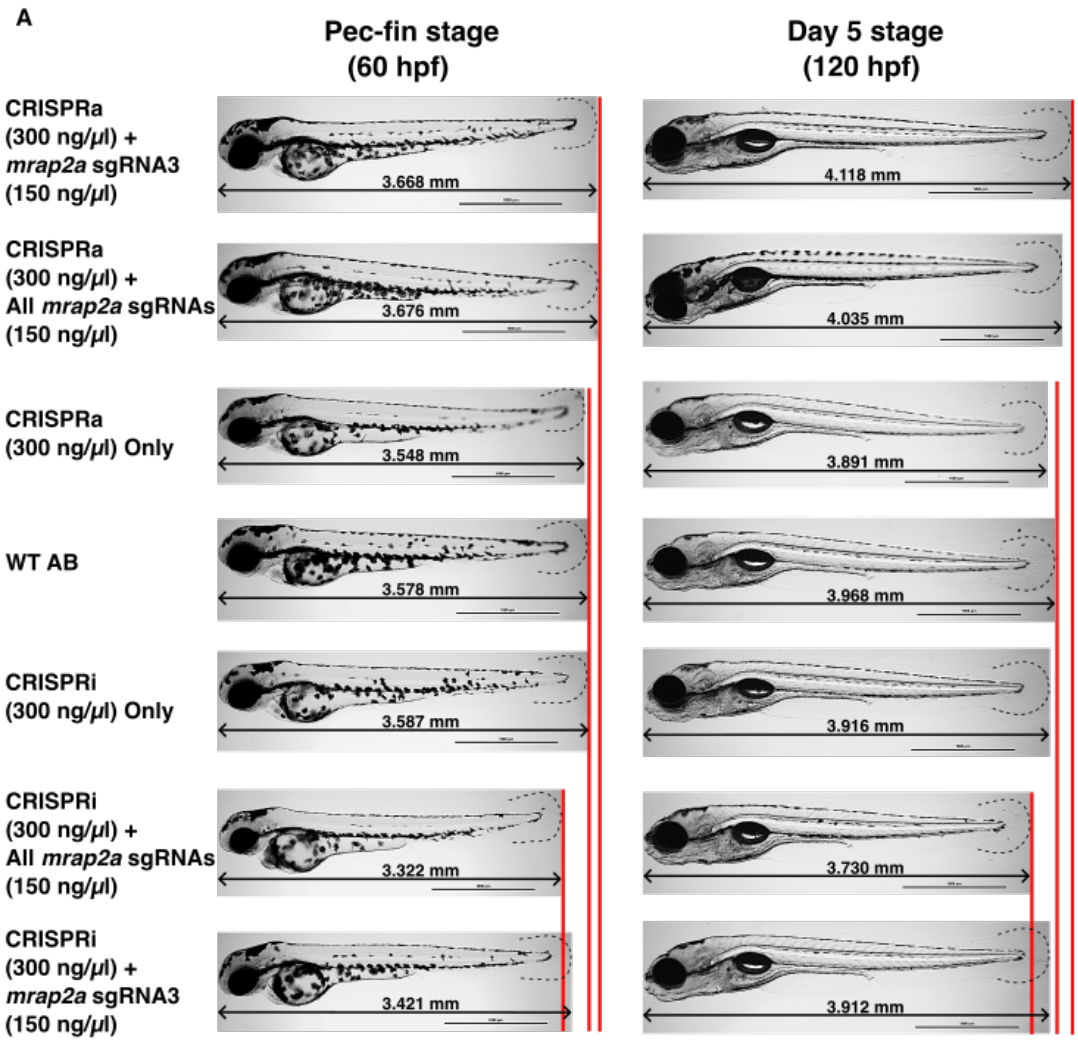
A
Pec-fin stage
(60 hpf)
Day 5 stage
(120 hpf)
CRISPRa
(300 ng/µl) +
mrap2a sgRNA3
(150 ng/µl)
3.668 mm
4.118 mm
CRISPRa
(300 ng/µl) +
All mrap2a sgRNAs
(150 ng/µl)
3.676 mm
4.035 mm
CRISPRa
(300 ng/µl) Only
3.548 mm
3.891 mm
WT AB
3.578 mm
3.968 mm
CRISPRi
(300 ng/µl) Only
3.587 mm
3.916 mm
CRISPRi
(300 ng/µl) +
All mrap2a sgRNAs
(150 ng/µl)
3.322 mm
3.730 mm
CRISPRi
(300 ng/µl) +
mrap2a sgRNA3
(150 ng/µl)
3.421 mm
3.912 mm

679

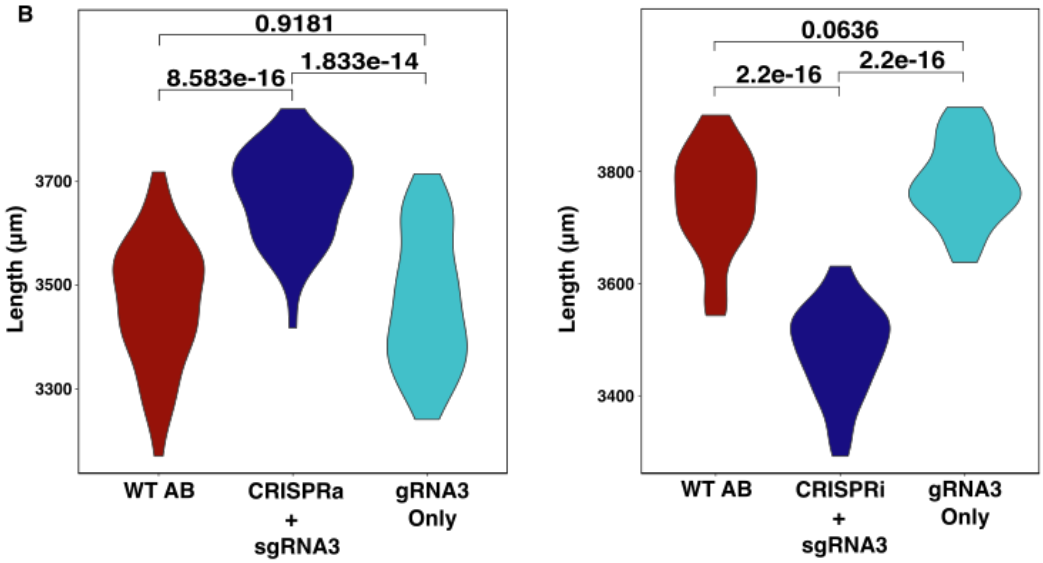
B
0.9181
8.583e-16
1.833e-14
Length (µm)
3700
3500
3300
WT AB
CRISPRa
+
sgRNA3
gRNA3
Only
0.0636
2.2e-16
2.2e-16
Length (µm)
3800
3600
3400
WT AB
CRISPRi
+
sgRNA3
gRNA3
Only

680

681 ***Figure 4:*** Targeting the promoter of *mrap2a* with CRISPRa and CRISPRi. **A.** Length comparison between
682 the pec-fin and day-5 stages between WT AB embryos and embryos injected with CRISPRa and
683 CRISPRi. Length measured laterally from tip of the head to end of fin tail (dashed lines). Red lines depict
684 length differences between controls and experimental conditions. Scale bars: 1000 μm. **B.** At the pec-fin
685 stage, 50 larvae per condition were measured in length and compared. The Welch two-sample t-test was
686 used to compare the average length between conditions.

687